

Quality Evaluation of Arbitrary Style Transfer: Subjective Study and Objective Metric

Hangwei Chen, Feng Shao, Xiongli Chai, Yuese Gu, Qiuping Jiang,
Xiangchao Meng, Yo-Sung Ho, *Fellow, IEEE*,

Abstract—Arbitrary neural style transfer is a vital topic with research value and industrial application prospect, which strives to render the structure of one image using the style of another. Recent researches have devoted great efforts on the task of arbitrary style transfer (AST) for improving the stylization quality. However, there are very few explorations about the quality evaluation of AST images, even it can potentially guide the design of different algorithms. In this paper, we first construct a new AST images quality assessment database (AST-IQAD) that consists 150 content-style image pairs and the corresponding 1200 stylized images produced by eight typical AST algorithms. Then, a subjective study is conducted on our AST-IQAD database, which obtains the subjective rating scores of all stylized images on the three subjective evaluations, i.e., content preservation (CP), style resemblance (SR), and overall visual (OV). To quantitatively measure the quality of AST image, we proposed a new sparse representation-based image quality evaluation metric (SRQE), which computes the quality using the sparse feature similarity. Experimental results on the AST-IQAD have demonstrated the superiority of the proposed method. The dataset and source code will be released at <https://github.com/Hangwei-Chen/AST-IQAD-SRQE>

Index Terms—Arbitrary style transfer (AST), Image quality assessment (IQA), Content preservation (CP), Style resemblance (SR), Overall visual (OV), Sparse coding, Sparse feature similarity.

I. INTRODUCTION

STYLE transfer is a process that strives to render natural images with particular style characteristics from one image (the style image) while synchronously maintaining the detailed structure information of the content image. This unique technique not only builds a bridge between the computer vision and appealing artworks, but also gets rid of the dilemma that it would take a long time for a well-trained artist to draw an image in a special style [1].

Early works [2], [3] cope with the style transfer using local statistics or similarity measures on the pixel values. Recently, the field of Neural Style Transfer (NST) was ignited by the groundbreaking work of Gatys et al. [4], which is the process of using Convolutional Neural Network (CNN) to perform image translation and stylization. Then, lots of follow-up studies were conducted to improve the NST algorithm based

on the deep neural network in order to promote the transfer efficiency and generation effects. Meanwhile, NST also has rapidly evolved from single-style to infinite-style models, also known as Arbitrary Style Transfer (AST) [5]–[28]. With the ability of utilizing one model to transfer arbitrary artistic style, AST has become a hot topic on computer vision, which could guild the creation of artworks and promote social communication. However, lacking of a good quantitative evaluation makes it difficult to measure the merits and drawbacks of the AST algorithms. It is therefore necessary to study and eventually evaluate the AST images.

A. Style Transfer Techniques

Mathematically, the style transfer model can be described as a translation process [29]:

$$I_{AB} \in B : \mathcal{M}_{A \rightarrow B}(I_A). \quad (1)$$

where I_A is the input content image from a source domain A to a target domain B , $\mathcal{M}_{A \rightarrow B}$ is a mapping that generates image $I_{AB} \in B$ indistinguishable from style image $I_B \in B$ on the target domain given the input source image $I_A \in A$.

Following the growth of neural networks, numerous NST methods have been proposed to study the problem of style transfer. According to the optimization ways adopted in the NST task, the existing NST methods can be divided into two categories: Image-Optimization-Based Online Neural Methods [8]–[12] and Model-Optimization-Based Offline Neural Methods [18]–[28], [30]–[32]. The former category could produce appealing stylized results through the iterative image optimization process, while the latter uses generated models with feed-forward networks to produce special style patterns. Particularly, considering the efficiency issue, it is more meaningful to design the Model-Optimization-Based Offline Neural Methods in practice.

The AST method is one of the Model-Optimization-Based Offline Neural Methods, which can accept an arbitrary artistic style as input and produce stylized results in a single feed-forward network once upon the model is trained. Thus, the AST has received substantial attention due to the increasing scientific and artistic values. In below, we review the details of the AST studies. For more comprehensive introduction, readers can refer to the survey [1].

1) *Non-Parametric Methods*: The common idea of the non-parametric methods [13]–[17] is to seek the similarities between the patches in content and style images and swap them. Chen et al. [14] realized AST for the first time that developed a Style-Swap operation to swap the feature patches of

Hangwei Chen, Feng Shao, Xiongli Chai, Yuese Gu, Qiuping Jiang, and Xiangchao Meng are with the Faculty of Information Science and Engineering, Ningbo University, Ningbo 315211, China (e-mail: 1010075746@qq.com; shaofeng@nbu.edu.cn; 747866472@qq.com; 805682724@qq.com; jiangqiuping@nbu.edu.cn; mengxiangchao@nbu.edu.cn).

Yo-Sung Ho is with the School of Information and Communications, Gwangju Institute of Science and Technology (GIST), Gwangju 500-712, Korea (e-mail: hoyo@gist.ac.kr).

content images with the best matching style feature patch-es. Another work by Gu et al. [15] also proposed a patch-based method which considered the matching of both global statistics and local patches. However, if the structures of content image and style image are different, these methods cannot efficiently protect the shape with unsatisfactory style patterns.

2) *Parametric Methods*: The characteristic of these parametric methods [18]–[28] is to optimize a target function that reflects the similarity between the input and stylized images. These parametric methods [18]–[22], [28] utilize the Gram-based VGG perceptual loss to produce stylization with a few modifications. Li et al. [22] proposed a linear transform function (LST) from content and style features for stylization. Li et al. [20] performed a pair of feature transforms, whitening and coloring (WCT), for feature embedding within a pre-trained encoder-decoder module. Huang et al. [19] proposed a novel adaptive instance normalization (AdaIN) layer that adjusts the mean and variance of the content input to match the style input. Another promising trend in parametric methods is to integrate attention mechanism into the deep neural network. Yao et al. [24] first considered multi-strokes with such self-attention framework. Park et al. [23] introduced Style-Attentional Network to match content and style features for achieving good results with evident style patterns. Deng et al. [27] proposed a multi-adaptation module that takes the global content structure and local style patterns into account. In addition, Zhang et al. [25] introduced a multi-modal style transfer (MST) via efficient graph cuts algorithms, which explicitly considers the matching of semantic patterns in content and style images. Inspired by MST, Chen et al. [26] developed a structure-emphasized multimodal style transfer (SEMST) model, which can flexibly match the content cluster and the style cluster based on the cluster center norm.

B. Image Quality Assessment of AST

1) *Motivations*: Notwithstanding the current state-of-the-art methods have shown successful stream in style transfer, arbitrary style transfer image quality assessment (AST-IQA) has been a long-standing problem and relatively unexplored in the community. Nevertheless, with the exception of a few quantitative protocols [33], [34], almost all researches evaluate the stylization quality in a qualitative way (e.g., by side-by-side subjective visual comparisons or different user studies), which suffers from the following limitations. First, the stylization examples displayed for qualitative comparison are few in number and often carefully selected by the researchers to favor the cases where the algorithm works well. In other words, the results of these presentations are not comprehensive enough. Second, the selected observers often lack sufficient experience and expertise, which makes qualitative evaluation less convincing. Thus, it is practical and necessary to propose a reliable metric for AST researchers to quantitatively assess the stylization quality.

2) *Challenges*: Different from the traditional IQA tasks [35]–[42] that usually focus on general distortions generated by various stimuli, the AST-IQA is closely related to aesthetics and poses serious challenges in both subjective and objective assessment.

Subjective assessment: The first challenge is how to design and conduct a human subjective study that can obtain reliable ground truth labeling on a set of stylized images [43]. To our best knowledge, there is no publicly available database for AST-IQA. The most related benchmarks are the non-photorealistic rendering (NPR) benchmarks [44], [45], which are used for testing stylization algorithms without human opinion scores. Currently, there is no quality assessment standard for measuring the performance of style transfer, since the AST-IQA is a highly subjective task, e.g., different subjects tend to have various ideas towards the same stylized result, especially for the style evaluation.

Objective assessment: Once the subjective dataset is obtained, the next challenge is how to design a metric that can automatically evaluate the perceptual quality of the AST images closely consistent to human vision. In several image style transfer works [29], [46], [47], some Full-reference (FR) metrics (e.g., structural similarity [48]) have been used to evaluate the similarity between the structures of the content and stylized images. However, strictly speaking, evaluating the AST quality is not a classic FR-IQA task. Straightforwardly applying the traditional FR-IQA strategy to the field of style transfer is problematic, since the stylized image has different detailed content information with the source and style images, and the ground truth image is unavailable for the stylized image (i.e., completely different with fidelity evaluation in the tradition IQA tasks). Although the general No-reference (NR) metrics (e.g., NIQE [42], BRISQUE [41] and BIQI [40]) have made great progress in the tradition IQA tasks without ground truth, they are also not applicable to AST-IQA because stylized images are closely related to aesthetics rather than naturalness. In addition, it is necessary for AST-IQA to fully take the original information of content and style images into account. Recent works target to address the challenges using some objective metrics from the perspective of different quality factors. Yeh et al. [33] proposed a quantitative metric with two factors (i.e., effectiveness and coherence), in which the former factor is a measure of the extent to which the style was transferred, and the latter is a measure of the extent to which the transferred image is decomposed into the content objects. Wang et al. [34] first decomposed the quality of style transfer into three quantifiable factors, i.e., the content fidelity (CF), global effects (GE) and local patterns (LP), which cover the main aspects considered by different types of existing NST methods. However, these objective metrics either focus on the limited factors of style transfer quality (e.g., lacking of fine-grained quality factors), or are simple in quality pooling, which cannot effectively match the aesthetic perception of human observers in practice.

C. Overview of Our Work

In this paper, to resolve the above challenges, we carry out an investigation for AST-IQA from both subjective and objective perspectives. With the popularization of art education, a majority of people with similar background can make similar perceptual judgments about some basic elements in artistic painting (e.g., color tone, brush stroke, distribution of objects,

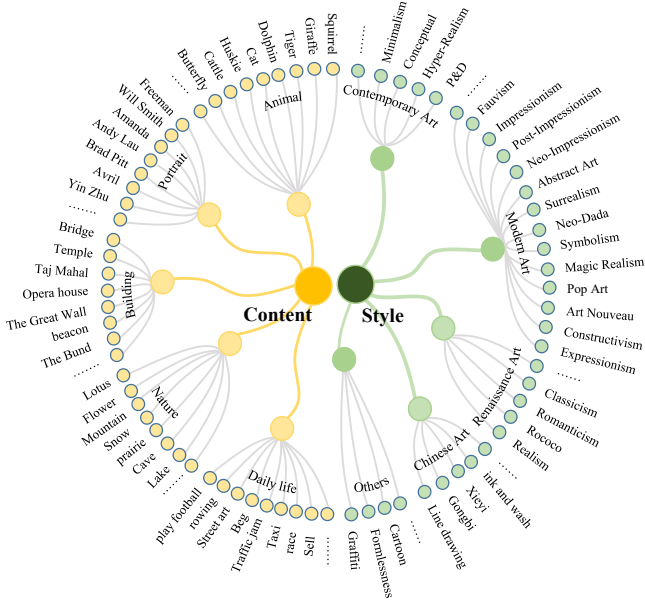


Fig. 1. Taxonomic structure of our source images.

and contents). Benefitted from the above conditions, to address the challenge in subjective assessment, we decompose the quality of AST into three quality factors that are easier to understand, namely content preservation (CP), style resemblance (SR), and overall visual (OV). These quality factors are assigned own preference labels by participants according to the knowledge in style transfer, intuition in vision and feedback from the surveys. To address the challenge in objective assessment, as suggested by the recommendation system [49], we regard the problem as a data-driven modeling of user preference [50], and conduct quantitative evaluation of AST-IQA using sparse representation to dig intrinsic representation for content and style images. To sum up, the major contributions of our work are summarized as follows:

1) To carry out in-depth study on perceptual quality assessment of AST stylized images from both subjective and objective aspects, we build a new AST images database named AST-IQAD, which consists 150 content-style image pairs and the corresponding 1200 stylized images produced by eight typical AST algorithms. Each stylized image contains the subject-rated CP, SR and OV scores. To our knowledge, it is the first large-scale AST image database with human opinion scores. Therefore, it can provide a benchmark to objectively evaluate the existing AST methods and potentially guide the design of different AST methods.

2) We proposed a new sparse representation-based image quality evaluation metric (SRQE) for AST-IQA, which can quantitatively evaluate the quality factors of CP, SR, and OV. To be more specific, in the training phase, we learn multi-scale style and content dictionaries to represent the style characteristic and structure of the stylized images. In the quality estimation phase, the sparse feature similarities are further exploited to compute the qualities of CP and SR respectively, and the OV quality is obtained by combining the

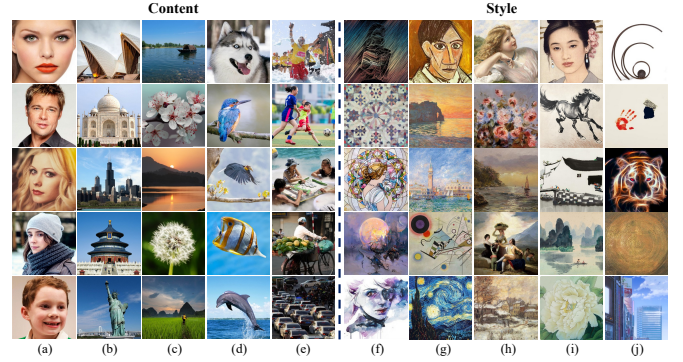


Fig. 2. Examples of content and style images in the AST-IQAD database. (a) Portraits. (b) Building. (c) Nature. (d) Animal. (e) Daily life. (f) Contemporary art. (g) Modern art. (h) Renaissance art. (i) Chinese art. (j) Others.

SR and CP qualities. Extensive experiments are conducted on the proposed AST-IQAD dataset and the experimental results demonstrate the proposed method can well evaluate the AST quality.

The rest of this paper is organized as follows. Section II illustrates the details of AST-IQAD. Section III introduces the proposed method in detail. The experimental results are shown and discussed in Section IV. Finally, conclusions are drawn in Section V.

II. AST-IQAD DATABASE

To investigate quality assessment of AST images, we construct a new arbitrary style transfer database (AST-IQAD) for quality assessment, which includes 1200 stylized images generated by eight typical AST methods, and conduct a subjective quality evaluation study on the AST-IQAD database to capture the human opinion scores. To our knowledge, it is the first large-scale database for AST-IQA, and it can provide a better resource to evaluate and advance state-of-the-art style transfer algorithms. We will introduce the details of the AST-IQAD database in the following parts.

A. Source Images

Since the essence of style transfer is to migrate the color tone and stroke pattern from the source to target image while retaining the content structure information of the target image. To provide deeper and intuitive information, the selected source images should have clear and reasonable structures. Thus, we set up a hierarchical taxonomic system (shown in Fig. 1) for source image (the content images) and target images (the style images), respectively. Both content and style images are labeled with five categories.

1) *Content Images*: We collect 75 high quality images with a resolution of 512×512 pixels from the NPRgeneral benchmark [44] and other famous photography websites. According to the criteria of coverage [44], the content images are comprised of five categories (i.e., animal, portrait, building, nature, and daily life) with a wide range of characteristics (e.g., contrast, texture, edges and meaningful structures). Examples of the selected content images in the database are shown in Fig. 2.

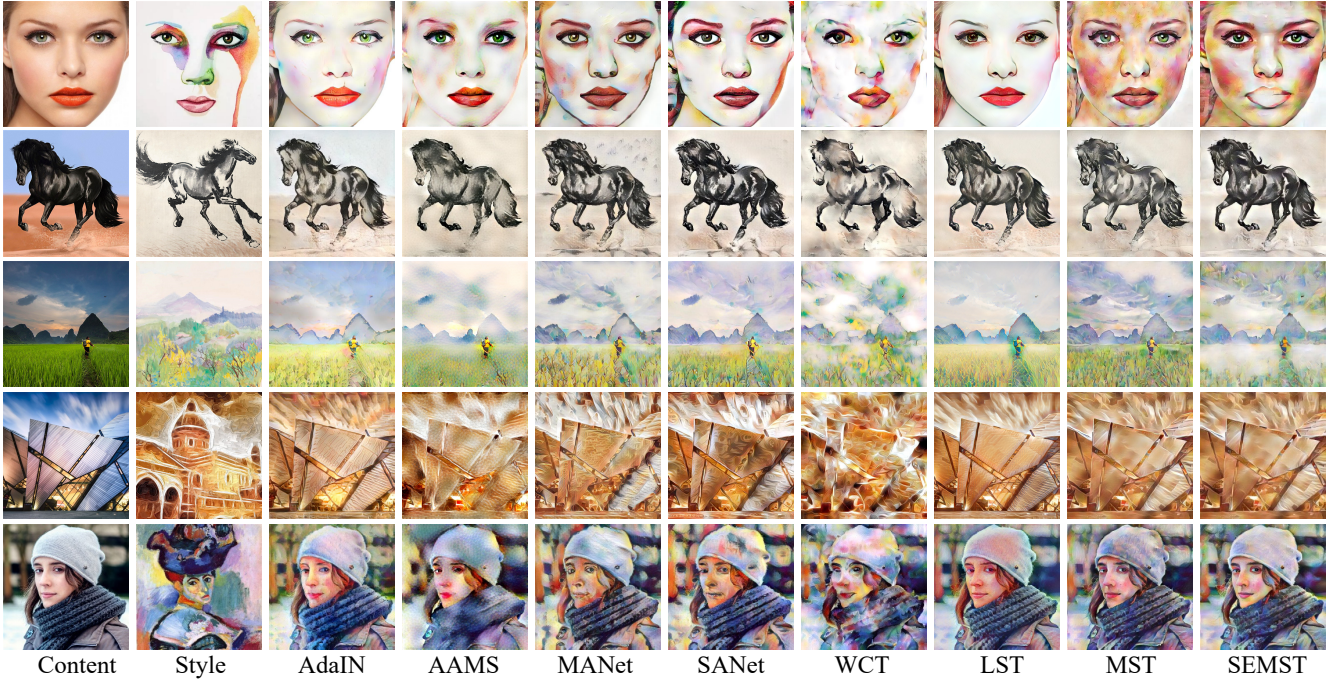


Fig. 3. Examples of AST images produced by different algorithms.

Quality	Choice criterion	Examples		Source Images
		✓	×	
CP	Ignoring the color and texture information, the structure and semantic information of the content image are more clearly preserved in the results.			
SR	Ignoring the content information, the color and stroke characteristics of the style image are more completely transferred to the result.			
OV	Depending on the type of style image, the style characteristics and content structure are better balanced in the result image.			

Fig. 4. Preference criteria for the AST-IQA task.

TABLE I
DESCRIPTION OF AST ALGORITHMS USED IN THE DATABASE.

Types	Methods	Descriptions
Gram-based	WCT [20]	Whitening and coloring transforms
	AdaIN [19]	Adaptive instance normalization
	LST [22]	Linear style transfer
Attention-based	AAMS [24]	Attention-aware Multi-stroke style transfer
	MANet [27]	Multi-adaptation networks
	SANet [23]	Style-attentional networks
Graph-based	MST [25]	Multimodal style transfer via graph cuts
Cluster-based	SEMST [26]	Structure-emphasized multimodal style transfer

2) *Style Images*: We select 126 style images with a resolution of 512×512 pixels, which cover five categories including

contemporary art, modern art, renaissance art, Chinese art, and others. The style images are downloaded from the WikiArt, which is the largest art encyclopedia in the visual arts from all over the world. Examples of style images in the AST-IQA dataset are also shown in Fig. 2.

3) *Content-Style Image Pairs*: Pairing content images with appropriate and diverse style images can make the AST results more aesthetically pleasing. In our work, we provide two mechanisms [11] of ‘Paired’ and ‘Unpaired’ for each content image, in which ‘Paired’ means that the content and the style images are semantically consistent (e.g., the same source of birds), while ‘Unpaired’ means that the content and the style images are the representations of different sources (e.g., the style images may be regular patterns or texture decorations). In total, we use 75 content images and 126 style images (including reused style images) to generate 150 content-style image pairs. Then, different AST algorithms are conducted on the content-style image pairs to generate the AST images. More information of the image pairs can be found in our database.

B. Arbitrary Style Transfer Algorithms

Different with traditional IQA databases that stimulated with different distortion stimuli, the testing images in our databases are generated from different AST methods. The eight representative AST methods used in the database are listed in Table I, including AAMS [24], AdaIN [19], MANet [27], LST [22], WCT [20], MST [25], SEMST [26], SANet [23]. These algorithms cover a wide variety of techniques, including Gram-based, Attention-based, Graph-based and Cluster-based methods. As a result, we can obtain 1200 style transferred images from 150 content-style image pairs. As shown by the examples

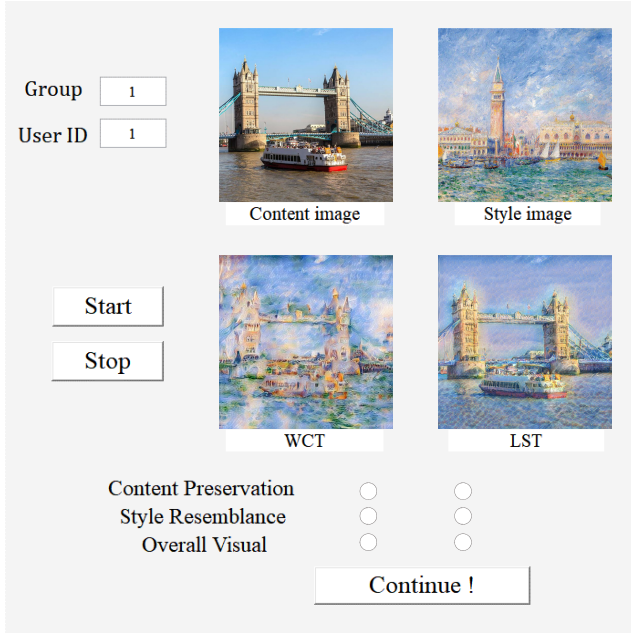


Fig. 5. Subjective interface in the experiment.

of style transferred images generated by eight different AST methods in Fig. 3, we have the following observations: 1) In the Gram-based methods, LST [22] and AdaIN [19] can well preserve the content information but may suffer from wash-out artifacts. On the contrary, WCT [20] is impressive in color and texture making the “painting taste” more intense while fails to preserve the main content structures. 2) The attention-based methods have distinct content structures and rich style patterns but may produce unpleasing visual artifacts. For example, SANet [23] and MANet [27] methods produce unpleasing eye-like artifacts, and AAMS [24] introduces imperceptible dot-wise artifacts. 3) The results of MST [25] and SEMST [26] are similar and produce both visible content and proper stylization.

C. Human Subjective Study

Due to the different rating standards across different observers and the influence of visual content [51], the subjective quality scores evaluated by absolute category rating are imprecise, biased, and inconsistent, while the preference label, representing the relative quality of two images, is generally precise and consistent for the task. For this consideration, we adopt the pairwise comparison (PC) approach which aims to provide a binary preference label between a pair of stylized images.

The experiment was carried out in a laboratory designed for human subjective study. The subjective software interface as shown in Fig. 5 is displayed on a 23-inch true color (32bits) LCD monitor calibrating in accordance with the ITU-R BT.500-13 recommendations [52]. In the interface specific to the AST task, participants are shown two stylized images along with a style-content image pair, and are required to vote on three preferences for content preservation (CP), style

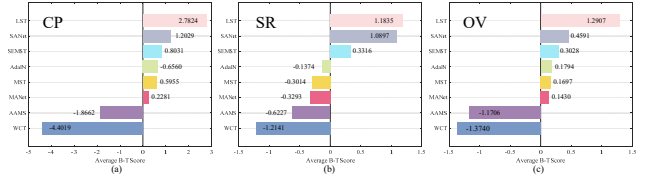


Fig. 6. Average B-T scores of different AST algorithms at each subjective evaluation.

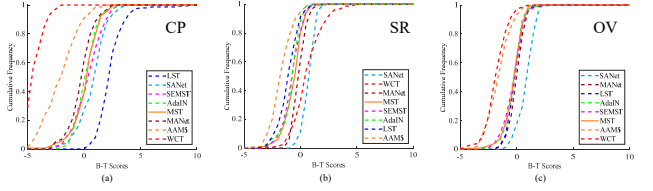


Fig. 7. Cumulative probability distribution curves of B-T scores at each subjective evaluation.

resemblance (SR), and overall visual (OV). The detailed descriptions of preference criteria are summarized in Fig. 4.

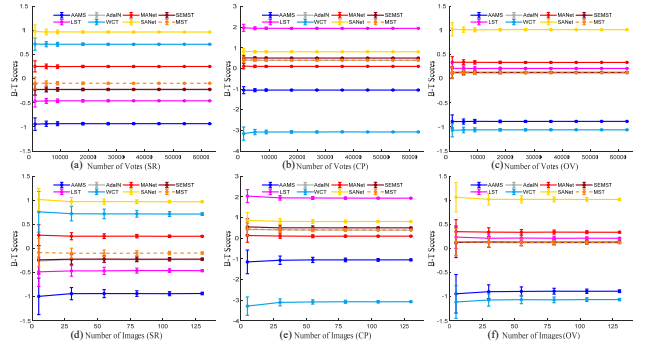


Fig. 8. Convergence analysis on the number of votes and image pairs at each subjective evaluation.

A total number of 45 subjects aged from 18 to 30, including experts and students from the Faculty of Art, and under-graduate students with experience in image processing, were participated in the subjective study. For each content-style image pair producing eight 8 AST results, we have 28 pairwise comparisons in the subjective ranking study. In total, 4200 pairwise comparisons from 150 content-style pairs are involved in the subjective study. To reduce the possible fatigue effect, we divide the experiment into three sub-sessions, in which each participant takes part in one sub-session completing 1400 PC voting within 4 hours. As a result, we can get 63,000 votes on each subjective evaluation.

D. Subjective Data Analysis

1) *Global Ranking of AST Algorithms*: To derive globally ranking of the AST algorithms from the corresponding PC results, we adopt the Bradley-Terry [53] model to estimate the subjective score for each algorithm. The probability that the i -th method is favored over the j -th method is defined as:

$$P(i \succ j) = \frac{e^{u_i}}{e^{u_i} + e^{u_j}}. \quad (2)$$

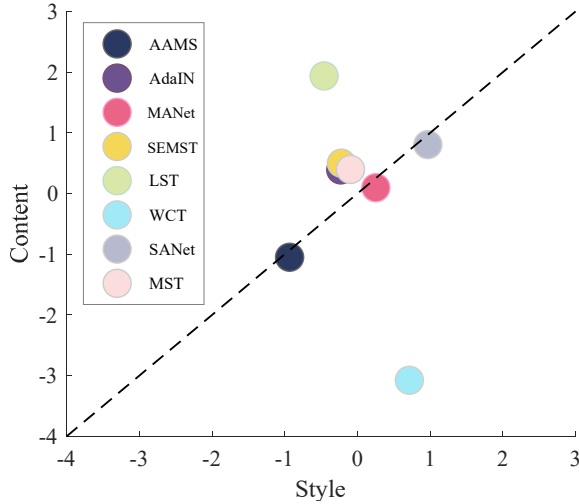


Fig. 9. Correlation of B-T scores between the subjective evaluations of CP and SR.

where u_i and u_j are subjective scores for the i -th and the j -th methods, respectively. Then, the negative log-likelihood for the B-T scores $\mathbf{u} \in \mathbb{R}^{n_{ast}}$, where n_{ast} is the number of AST algorithms, can be jointly expressed as:

$$\mathcal{L}(\mathbf{u}) = -\log \left(\prod_{i=1}^{n_{ast}} \prod_{j=1, j \neq i}^{n_{ast}} P(i \succ j)^{\mathcal{W}_{ij}} \right) \quad (3)$$

where \mathcal{W}_{ij} is the (i, j) -th element in the winning matrix $\mathcal{W} \in \mathbb{Z}^{n_{ast} \times n_{ast}}$, representing the number of times that the i -th method is preferred over the j -th method. By setting the derivative of $\mathcal{L}(\mathbf{u})$ in Eq. (3) to zero to solve the optimization problem [54], the final B-T scores \mathbf{u} are obtained via zero mean normalization, served as the ground truth subjective rating scores. We can get a B-T score for each AST result in each sub-session by applying the B-T model. Fig. 6 shows the average B-T scores of different AST methods for three subjective evaluations (i.e., CP, SR, and OV). A higher B-T score indicates a better performance. From the figure, some interesting observations could be drawn: 1) The B-T scores of different AST algorithms show various trends on the subjective evaluations of CP, SR and OV, which indicate that different methods have specific advantages. 2) For the CP evaluation, LST [22], which receives the best ranking, has shown significant advantage in maintaining structure information over other methods by a large margin. WCT [20] performs worst in the CP test due to treating diverse image regions in an indiscriminate way. 3) For the SR evaluation, SANet [23] performs best on average, attributed to the attention mechanism that generates more local style details. However, AAMS [24], which is also based on self-attention mechanism, does not perform well because the multi-stroke pattern generates imperceptible dot-wise artifacts. In addition, WCT [20] shows the competitive advantage, which indicates the effectiveness of whitening and coloring transformations. 4) For the OV evaluation, attention-based methods (e.g., SANet [23] and MANet [27]) rank top-2 on performance. It is not surprising because attention-based algorithms pay more attention to those

feature-similar areas in the style image for stylizing a content image region. Furthermore, we plot the cumulative probability distribution curves of the B-T scores obtained from all AST results in Fig. 7. The AST method corresponding to the rightmost curve performs better because it accumulates higher B-T scores.

2) *Convergence Analysis*: To demonstrate that the scale of the subjective study is large enough to support performance evaluation, we further analyze the convergence from the perspectives of the number of subject votes and images pairs [51].

Number of votes: We randomly sample λ ($\lambda = 10000, 20000, \dots, 60000$) votes from a total of 63,000 voting results, and calculate the B-T scores for each AST algorithm. To avoid the possible bias, we repeat this process 1000 times with different samples of votes. Fig. 8 (a)-(c) show the mean and standard deviation of B-T scores for each sample at three subjective evaluations. It is observed that as the number of votes grows, the B-T scores tend to be stable, which demonstrates that the number of votes is sufficiently large for performance evaluation.

Number of images pairs: Similar to the above convergence analysis, we randomly sample μ ($\mu = 20, 50, 75, 100, 125$) content-style image pairs from our dataset and then plot the means and the standard deviations in Fig. 8 (d)-(f). Obviously, as the number of images pairs grows, standard deviation of B-T Scores decreases, which indicates that the B-T scores obtained from the subjective study are stable.

Overall, the above two kinds of convergence analysis demonstrate the reliability and stability of the subjective rating scores.

3) *Correlation of B-T Scores*: This part analyzes the correlation of B-T scores between the CP and SR evaluations, as shown in Fig. 9. The method above (below) the diagonal indicates better performance in CP (SR), and vice versa. From the figure, it is observed that the SANet [23] method has achieved a better consistency in SR and CP evaluation, and the WCT [20] method shows excellent performance in SR but fails to sufficiently maintain the content structure.

III. OBJECTIVE QUALITY EVALUATION

In this paper, we proposed a new sparse representation-based image quality evaluation metric (SRQE) for AST-IQA, as shown in Fig. 10. The process is composed of two phases: multi-scale dictionary training and quality estimation. In the training phase, the multi-scale style and content dictionaries, learnt from the training databases via sparse representation, are utilized to build style representation for style images and capture inherent structures for the content images, respectively. In the quality estimation phase, the quality of SR (or CP) is obtained by estimating the sparse feature similarity between the stylized image and the style (or content) image. Finally, the OV quality is obtained by combining the SR quality and CP quality together. In what follows, we elaborate on each step of the proposed method.

A. Style Feature Extraction

1) *Selection of Training Database*: As show in Fig. 11 (a), we re-collected 100 new style images, covering a wide variety

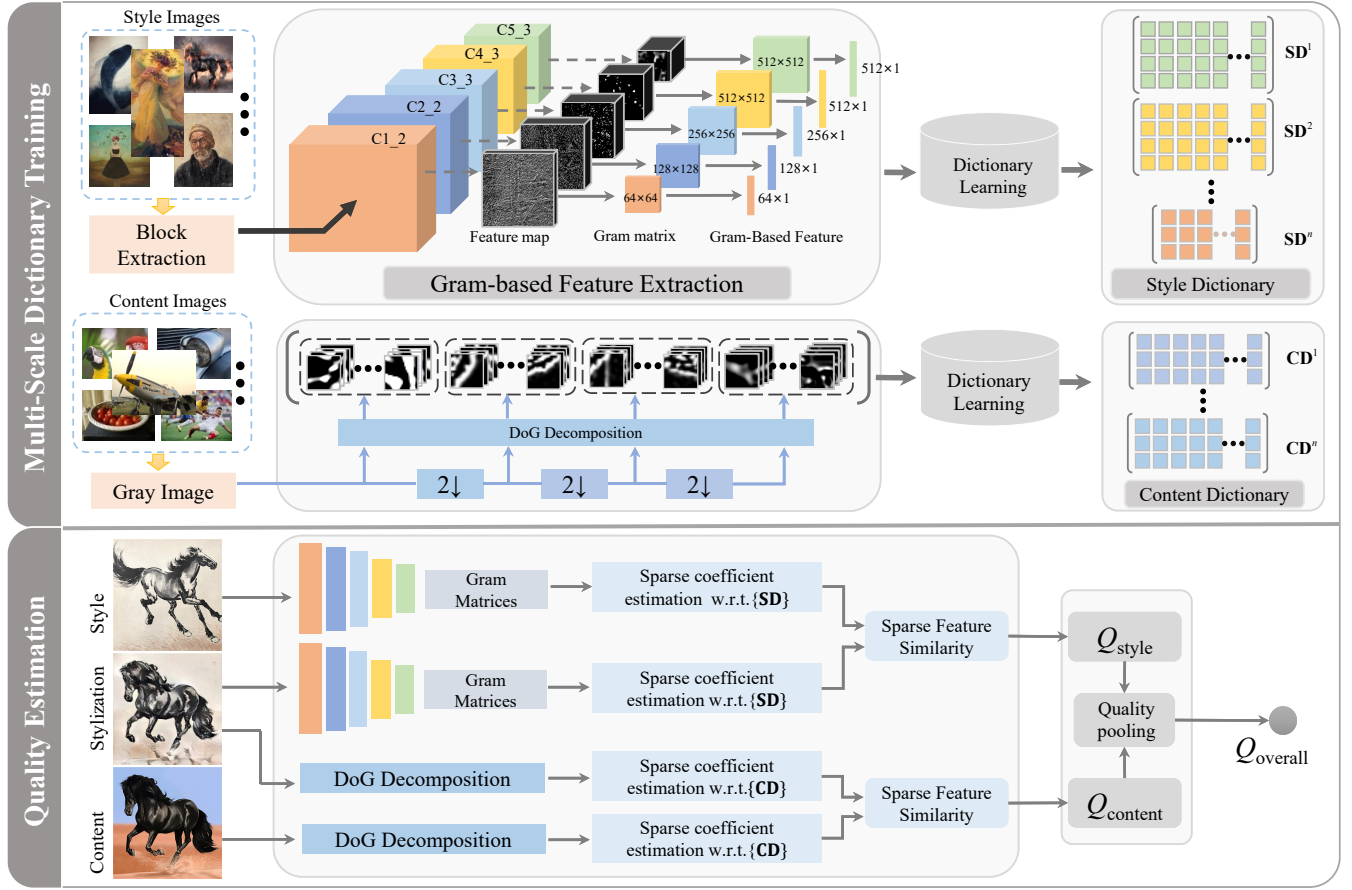


Fig. 10. Framework for the proposed sparse representation-based method.

of categories, as training images for dictionary learning. Note that there is no overlap between these images and the above collected style images (in the Section II-A) to ensure the complete independence of the training and test data. In addition, we augment the training database by cropping the images to reduce overfitting.

2) *Gram-Based Feature*: The work in [4] demonstrated that the correlations between convolution responses at the same layer (i.e., Gram matrices) yielded effective texture synthesis and can effectively grasp the image style. Additionally, sparse representation technique shows great prospects in image visual style analysis [55]. Inspired by this, we construct a style perception model based on sparse representation, while incorporating high-level perceptual information (Gram matrices) extracted from deep neural network. In this paper, we resort to compute gram matrices from style images using a pre-trained VGG network of the state-of-the-art full-reference IQA model (DISTS) [56] which has superior performance in evaluating texture similarity. Assumed that the feature map of a sample style image I_s at layer l of DISTS [56] is denoted as $\mathbf{F}^l(I_s) \in \mathbb{R}^{C \times H \times W}$, where C is the number of channels, and H and W represent the height and width of the feature map, the Gram-based representation is computed from the feature map $\mathbf{F}^l(I_s)' \in \mathbb{R}^{C \times (HW)}$ aggregated from

the $\mathbf{F}^l(I_s) \in \mathbb{R}^{C \times H \times W}$:

$$\mathbf{G}(\mathbf{F}^l(I_s)') = [\mathbf{F}^l(I_s)'] [\mathbf{F}^l(I_s)']^T \quad (4)$$

In the implementation, we use the first to fifth VGG network layers of DISTS [56] to produce a set of Gram-based representations at different layers, namely $\{\mathbf{G}^l \in \mathbb{R}^{C \times C}, l = 1, 2, \dots, L\}$, where $L=5$ denotes the highest layer and $C \in \{64, 128, 256, 512, 512\}$ correspond to the numbers of feature maps at each layer.

After the above processing, each Gram-based representation then generates a Gram-based style feature vector $\mathbf{g}^l \in \mathbb{R}^{C \times 1}$ through averaging each row, described as:

$$\mathbf{g}^l = \mathbf{G}^l \cdot \mathbf{x}^l. \quad (5)$$

$$\mathbf{x}^l = [x_1^l, x_2^l, \dots, x_C^l]^T. \quad (6)$$

where $x_1^l = \dots = x_C^l = 1/C$

Finally, numerous style feature vectors at the same layer extracted from different style images are used to form a style matrix \mathbf{SM} . As a result, we can obtain five different style matrices (corresponding to five layers) $\mathbf{SM}^l = [\{\mathbf{g}^l\}_1, \{\mathbf{g}^l\}_2, \dots, \{\mathbf{g}^l\}_{N^l}] \in \mathbb{R}^{C \times N^l}$. All style matrices will be used for the subsequent style dictionary learning.

3) *Multi-Scale Style Dictionary Learning*: Using the above style matrices $\mathbf{SM}^l = [\{\mathbf{g}^l\}_1, \{\mathbf{g}^l\}_2, \dots, \{\mathbf{g}^l\}_{N^l}] \in \mathbb{R}^{C \times N^l}$ as input, we learn multi-scale style dictionary \mathbf{SD}^l by seeking



Fig. 11. Some of the images of the training databases used in the paper. (a) Style training database. (b) Content training database.

a sparse representation for each style feature vector \mathbf{g}^l under specific sparsity constraint τ . Each style sub-dictionary $\mathbf{SD} = [\mathbf{sd}_1, \mathbf{sd}_2, \dots, \mathbf{sd}_U] \in \mathbb{R}^{C \times U}$ contains U basic elements. Formally, the process of multi-scale style dictionary learning can be formulated as:

$$\begin{aligned} \langle \mathbf{SD}^l, \hat{\alpha}_i \rangle = \arg \min \sum_{i=1}^N \left\| \{\mathbf{g}^l\}_i - \mathbf{SD}^l \alpha_i \right\|_2^2 \\ \text{s.t. } \forall i, \|\alpha_i\|_0 \leq \tau \end{aligned} \quad (7)$$

where $\|\cdot\|_2$ is the l_2 -norm operator, $\|\cdot\|_0$ denotes the l_0 -norm that counts the number of non-zero elements in a vector, and α_i is the sparse coefficient vector of $\{\mathbf{g}^l\}_i$. Typically, both \mathbf{SD}^l and α_i are unknown in this stage. We resort to the online dictionary learning (ODL) algorithm implemented in the SPArse Modeling Software [57] to solve this NP-hard problem. Details of dictionary learning can refer to [57].

B. Content Feature Extraction

1) *Selection of Training Database*: Since the essence of the proposed content evaluation model is to restore the structure information of the source content images and stylized images based on dictionary learning, we only select natural images to construct the content dictionary. Refer to [58], we randomly select ten natural images from the TID 2013 [59] Database and NPRgeneral [44], which have different scenes in the images, as shown in Fig. 11 (b).

2) *DoG Response Feature*: As known, human visual perception is highly sensitive to the edge information, the major objects in the painting emphasized by the artists often contain distinct edges in most cases [50]. Intuitively speaking, the outline of the main objects largely reflects the content information of artworks. Inspired by this, the edge information, as the significant component in painting content, needs to be deeply investigated for evaluating the CP quality. Furthermore, an outstanding painting will be appreciated by humans at different distances. Thus, it is necessary to utilize multi-scale space to better describe the content of the painting from coarse level to fine level [60]. Hence, the multi-scale Difference of Gaussian (DoG) is applied to represent the image content feature [61], [62], which can properly simulate the receptive field of retinal cells.

First, the DoG signals, $DoG(x, y)$, at different scales can be computed by:

$$DoG(x, y) = |R_{\sigma, k\sigma}(x, y) \otimes I(x, y)|. \quad (8)$$

where $I(x, y)$ denotes the pixel location (x, y) of the input image, the symbol \otimes denotes the convolution operation, and $R_{\sigma, k\sigma}(x, y)$ is defined as the difference between two Gaussian kernel with nearby scales σ and $k\sigma$:

$$\begin{aligned} R_{\sigma, k\sigma}(x, y) = \frac{1}{2\pi\sigma^2} \exp\left(-\frac{x^2 + y^2}{2\sigma^2}\right) \\ - \frac{1}{2\pi k^2\sigma^2} \exp\left(-\frac{x^2 + y^2}{2k^2\sigma^2}\right) \end{aligned} \quad (9)$$

where σ and k are used to control the scales of DoG. Refer to [58], we set $k = 1.6$, and $\sigma \in \{0, 1, 1.6, 2.56, 4.096\}$ in the experiment. Here, $\sigma = 0$ denotes the original scale.

Once the DoG signals at the current octave are computed, the last scale-space image was selected as the new input and was down-sampled by a factor of two to repeat the above process, thereby producing a set of DoG signals with a variety of octaves and scales, namely $\{DoG^{z,o}(x, y)\}$, where $z \in \{1, \dots, Z\}$ denotes the z -th scale, and $o \in \{1, \dots, O\}$ denotes o -th octave.

After the above processing, each DoG signal is partitioned into numerous patches with size of 8×8 , subtracted by the mean value. In the implementation, 1000 overlapped patches having rich details and structures are selected as training samples. Then, these patches are vectorized into column vectors to form a content matrix \mathbf{CM} , $\mathbf{CM} = [\mathbf{y}_1, \dots, \mathbf{y}_k] \in \mathbb{R}^{T \times K}$, based on which the subsequent overcomplete content dictionary is learned. Each patch $\mathbf{y}_k \in \mathbb{R}^{T \times 1}$ contains T pixels and $k = 1, \dots, K$. Here, $K = 1000$.

3) *Multi-Scale Content Dictionary Learning*: Similar to the above multi-scale style dictionary learning, the multi-scale content dictionary $\mathbf{CD}^{z,o}$ can be learned from multi-scale content matrices $\mathbf{CM}^{z,o}$. Each content sub-dictionary $\mathbf{CD} = [\mathbf{cd}_1, \mathbf{cd}_2, \dots, \mathbf{cd}_V] \in \mathbb{R}^{C \times V}$ contains V basic elements. In the experiment, we set $V = 256$. Similarly, the process of multi-scale content dictionary learning can be formulated as:

$$\begin{aligned} \langle \mathbf{CD}^{z,o}, \hat{\beta}_i \rangle = \arg \min \sum_{i=1}^K \left\| \mathbf{y}_i - \mathbf{CD}^{z,o} \beta_i \right\|_2^2 \\ \text{s.t. } \forall i, \|\beta_i\|_0 \leq \tau \end{aligned} \quad (10)$$

where β_i is the sparse coefficient vector of \mathbf{y}_i . Note that we also apply the ODL algorithm to solve Eq. (10).

C. Feature Similarity Measurement

Through the above efforts, we obtained two types of over-complete multi-scale dictionaries, containing U and V basic atoms as the column vectors in \mathbf{SD}^l and $\mathbf{CD}^{z,o}$, respectively. Thus, each style feature vector \mathbf{g}^l (or content patch \mathbf{y}_k) can be sparsely represented as a linear combination of basic atoms contained in \mathbf{SD}^l (or $\mathbf{CD}^{z,o}$).

1) *Style Sparse Coefficients Estimation*: Given the testing stylized image I_t and style image I_s , we can obtain two Gram-based representations using the DISTS network, denoted as $\mathbf{G}_t^l \in \mathbb{R}^{C \times C}$ and $\mathbf{G}_s^l \in \mathbb{R}^{C \times C}$. Then, the style sparse

coefficient vectors can be estimated by a weighted linear combination of previously learnt dictionary elements, i.e.,

$$\mathbf{s}^l = \mathbf{G}_s^l \times (\mathbf{SD}^l)^+ \quad (11)$$

$$\mathbf{ts}^l = \mathbf{G}_t^l \times (\mathbf{SD}^l)^+ \quad (12)$$

where $(\mathbf{SD}^l)^+$ denotes the generalized inverse matrices of (\mathbf{SD}^l) .

2) *Content Sparse Coefficients Estimation*: For the testing stylized image I_t and the source content image I_c , after the same processing steps as in the training phase, we can obtain patch vectors $\mathbf{y}_c^{z,o}$ from I_c and its corresponding patch vectors $\mathbf{y}_t^{z,o}$ from I_t . Similarly, the content sparse coefficient can be computed by:

$$\mathbf{c}^{z,o} = \mathbf{y}_c^{z,o} \times (\mathbf{CD}^{z,o})^+ \quad (13)$$

$$\mathbf{tc}^{z,o} = \mathbf{y}_t^{z,o} \times (\mathbf{CD}^{z,o})^+ \quad (14)$$

where $(\mathbf{SD}^l)^+$ denote the generalized inverse matrices of (\mathbf{SD}^l) .

3) *Sparse Feature Similarity Measure*: From the above estimation phase, we generate the sparse coefficients $\mathbf{s}^l, \mathbf{c}^{z,o}, \mathbf{ts}^l, \mathbf{tc}^{z,o}$ on style, content and stylized images. Considering that these sparse coefficients were represented as a linear combination of basis vectors, meaning that the similarity between the style feature vectors or content patches can be directly measured using their sparse coefficient vectors. Thus, the style and content similarities are respectively defined as:

$$SS^l[\mathbf{G}_s^l, \mathbf{G}_t^l] = \frac{2 \langle \mathbf{s}^l, \mathbf{ts}^l \rangle + \eta}{\|\mathbf{s}^l\|_2 \cdot \|\mathbf{ts}^l\|_2 + \eta} \quad (15)$$

$$CS^{z,o}[\mathbf{y}_c^{z,o}, \mathbf{y}_t^{z,o}] = \frac{2 \langle \mathbf{c}^{z,o}, \mathbf{tc}^{z,o} \rangle + \eta}{\|\mathbf{c}^{z,o}\|_2 \cdot \|\mathbf{tc}^{z,o}\|_2 + \eta} \quad (16)$$

where $\langle \cdot \rangle$ calculates the inner product, η is a constant with a small value added to prevent the denominator to be zero and is set as 0.02. The SS measures the style similarity between the style and the stylized image, and CS measures the content similarity between the content and the stylized image.

D. Final Quality Pooling

To measure the final quality between a stylized image and its corresponding content and style images, we need to pool the above spare feature similarities into a single score. In our pooling strategy, we first pool the style and content sparse feature similarities into SR and CP scores across all scales or octaves, and then combine the scores to measure the OV quality score. First, the SR quality score Q_{style} is defined as:

$$Q_{style} = \prod_{l=1}^L (SS)^l \quad (17)$$

Then, the CP quality score $Q_{content}$ is defined as:

$$Q_{content} = \frac{1}{Z^2} \prod_{o=1}^O \left(\sum_{z=1}^Z (CS)^{z,o} \right) \quad (18)$$

where Z and O denote the number of scales and octaves.

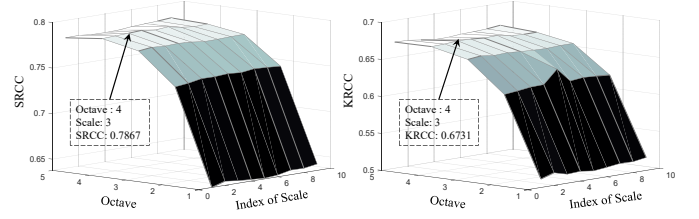


Fig. 12. Impacts of various octave and scale combinations on the performance of the $Q_{content}$ on CP evaluation.

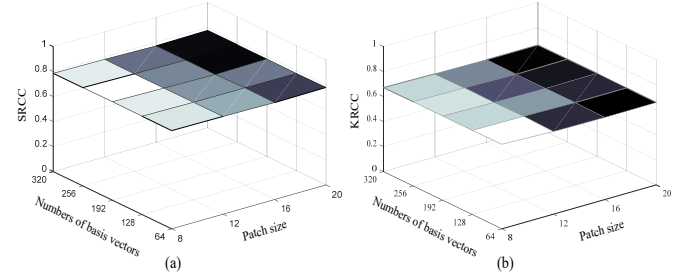


Fig. 13. Impacts of various patch sizes and numbers of basis vectors combinations on the performance of the $Q_{content}$ on CP evaluation.

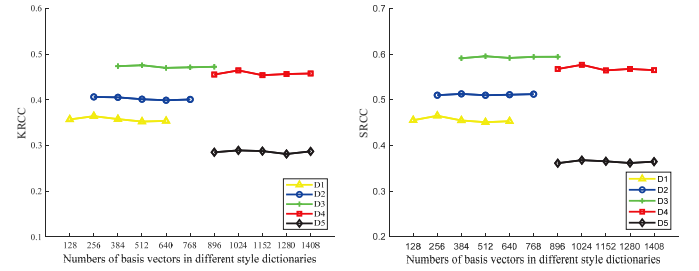


Fig. 14. Impacts of numbers of basis vectors on the performance of the Q_{style} on SR evaluation.

Finally, the OV quality $Q_{overall}$ is calculated by combining Q_{style} and $Q_{content}$ into a score:

$$Q_{overall} = (Q_{style})^{\omega_1} \cdot (Q_{content})^{\omega_2} \quad (19)$$

where the parameters ω_1 and ω_2 are used to adjust the relative importance of the two portions. For simplicity, we set $\omega_1 = \omega_2 = 1$ in this paper. Of course, there is a large room to manipulate the importance weights for better quality prediction. A more meaningful practice may be to explore the proper combination of Q_{style} and $Q_{content}$ that best fits human subjective study.

IV. EXPERIMENTAL RESULTS

A. Evaluation Criteria

Similar to [63], [64], two criteria are utilized for performance evaluation: the Spearman rank order correlation coefficient (SRCC) and Kendall Rank-order Correlation Coefficient (KRCC), which measure the prediction monotonicity. Considering that the ground truth B-T scores are only meaningful within the same group, these criteria are computed respectively for each group from the same source image. Then, the average

TABLE II
PERFORMANCE COMPARISON ON CP EVALUATION.

Method		Portrait		Building		Nature		Animal		Daily Life		All	
		KRCC	SRCC	KRCC	SRCC	KRCC	SRCC	KRCC	SRCC	KRCC	SRCC	KRCC	SRCC
FR-IQA	SSIM	0.5178	0.6282	0.5537	0.6664	0.4781	0.5884	0.5306	0.6460	0.6164	0.7561	0.5393	0.6570
	FSIM	0.5895	0.7141	0.5947	0.7154	0.5496	0.6642	0.5688	0.6924	0.6668	0.7903	0.5939	0.7153
	MS-SSIM	0.6706	0.7923	0.6637	0.7809	0.6070	0.7349	0.6404	0.7504	0.7000	0.8208	0.6563	0.7759
	IW-SSIM	0.6564	0.7736	0.6063	0.7272	0.5714	0.6953	0.5760	0.6984	0.6477	0.7748	0.6115	0.7339
	PSNR	0.3296	0.4150	0.4270	0.5389	0.3613	0.4570	0.4780	0.5860	0.5450	0.6766	0.4282	0.5347
	MAD	0.5705	0.6867	0.6117	0.7227	0.5616	0.6793	0.6117	0.7369	0.6547	0.7834	0.6020	0.7218
	VIF	0.6088	0.7384	0.5061	0.6248	0.4640	0.5909	0.5424	0.6769	0.5828	0.7214	0.5408	0.6705
	VSI	0.4793	0.5960	0.5875	0.7114	0.5926	0.7290	0.5473	0.6706	0.6257	0.7480	0.5665	0.6910
	GMSD	0.4846	0.5941	0.4589	0.5801	0.4878	0.6047	0.4401	0.5527	0.6167	0.7422	0.4976	0.6148
	UQI	0.2771	0.3682	0.4384	0.5323	0.2895	0.3949	0.3969	0.5045	0.4137	0.5265	0.3631	0.4653
	IFC	0.6112	0.7411	0.5395	0.6601	0.4760	0.6008	0.5401	0.6730	0.5805	0.7214	0.5494	0.6793
	RFSIM	0.4797	0.5878	0.5249	0.6485	0.4495	0.5606	0.5520	0.6932	0.6546	0.7802	0.5321	0.6541
	DISTS	0.5084	0.6323	0.6611	0.7773	0.5020	0.6389	0.5380	0.6734	0.6549	0.7795	0.5729	0.7003
$Q_{content}$		0.6659	0.7796	0.7093	0.8040	0.6166	0.7421	0.6449	0.7646	0.7286	0.8430	0.6731	0.7867

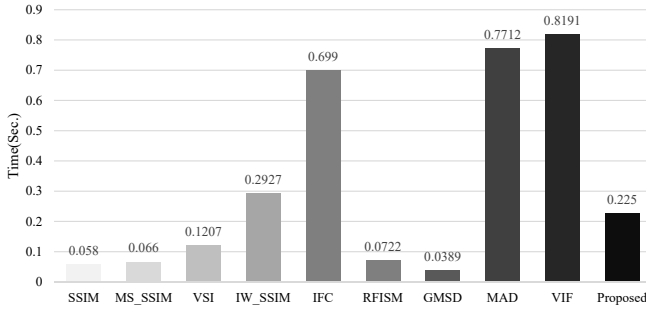


Fig. 15. Average execution time required for processing a stylized image with size 512×512 (in seconds).

value of all 150 groups is reported as the final performance score. A superior metric should have higher SRCC and KRCC values (with a maximum of 1).

B. Parameter Setting

Since the proposed quality metrics (i.e., Q_{style} , $Q_{content}$ and $Q_{overall}$) operate in a multi-scale framework containing several parameters, this section investigates the impacts of these parameters on subsequent quality evaluation.

1) *Parameters in $Q_{content}$* : For multi-scale content dictionary, we first visualize the influence of different combinations of scale and octave with at most 10 scales and 5 octaves on the performance of $Q_{content}$ in Fig. 12. It shows that the performance is greatly affected by the number of octaves while slightly affected by the number of scales. Here, we set the number of octaves $O = 4$ and the number of scales $Z = 3$, which can achieve the best performance. In addition, we tune the patch size and the number of basis vectors. As shown in Fig. 13, the evaluation accuracy is hardly affected by patch size and the number of basis vectors. In this work, we set $T = 64$ (patch size = 8) and $V = 256$.

2) *Parameters in Q_{style}* : For multi-scale style dictionary, since the Gram-based style feature vector of each layer is fixed, we only test the effect of the number of basis vectors. As shown in Fig. 14, the evaluation accuracy varies relatively slight over the numbers of basis vectors, which indicates that

TABLE III
PERFORMANCE COMPARISON ON SR EVALUATION.

Method	SRCC	KRCC
Q_{style}	0.6038	0.4847

TABLE IV
PERFORMANCE COMPARISON ON OV EVALUATION.

Method	SRCC	KRCC
Q_{SSIM}^*	0.5042	0.3905
Q_{FSIM}^*	0.5436	0.4405
$Q_{MS-SSIM}^*$	0.5761	0.4498
$Q_{IW-SSIM}^*$	0.5526	0.4298
Q_{PSNR}^*	0.4677	0.3726
Q_{MAD}^*	0.4962	0.3828
Q_{VIF}^*	0.4804	0.3619
Q_{VSI}^*	0.3948	0.3065
Q_{GMSD}^*	0.4175	0.3155
Q_{UQI}^*	0.3834	0.3004
Q_{IFC}^*	0.4763	0.3624
Q_{RFSIM}^*	0.3779	0.2801
Q_{DISTS}^*	0.5230	0.4084
$Q_{overall}$	0.5933	0.4734

the Q_{style} does not highly depend on the training configurations. In this paper, we set $U \in \{256, 256, 512, 1024, 1024\}$.

C. Performance Test on Different Quality Factors

1) *Performance Test on CP*: Although the evaluation of CP between the stylized images and source content images is not a classic FR-IQA problem, since the stylized image targets to maintain the structure information of source content image, the structure measurement module commonly included in existing FR-IQA methods is relatively suitable for comparison. As a consequence, we compare the proposed $Q_{content}$ with 13 state-of-the-art general-purpose FR-IQA metrics, including SSIM [48], FSIM [38], MS-SSIM [65], IW-SSIM [37], Peak Signal-to-Noise Ratio (PSNR), MAD [66], VIF [36], VSI [39], GMSD [67], UQI [68], IFC [69], RFSIM [70] and DISTS [56]. The performance comparison results are listed in Table II where the best metric is highlighted in red boldface. It can

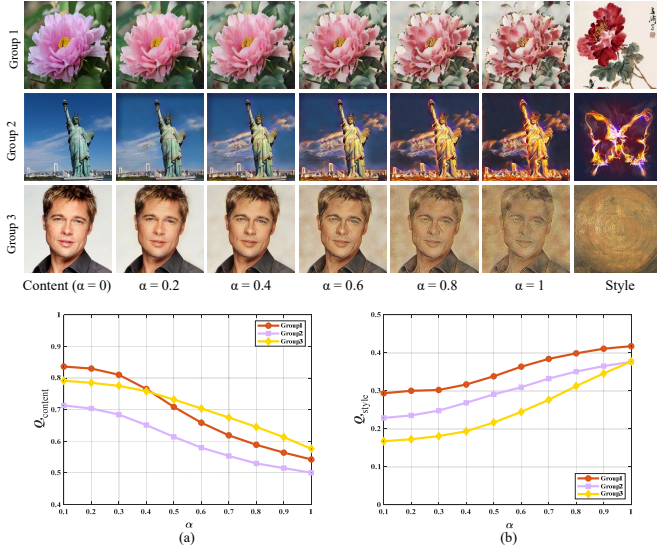


Fig. 16. Robustness analysis of the proposed Q_{style} and $Q_{content}$ in content and style trade-off application.

be seen that the $Q_{content}$ achieves the best performance on four subsets than the other metrics, but is slightly inferior than MS-SSIM [65] on portrait subset. Overall, the $Q_{content}$ achieves the best results in the average performance of five subsets, which demonstrates the effectiveness of $Q_{content}$ on CP evaluation.

Furthermore, we compare the time complexity of partial methods via running MATLAB codes (R2018a) on a PC with Intel (R) Core (TM) i5-8400M CPU at 2.8 GHz, 16 GB RAM, Windows 10 Pro 64-bit operation system. The average execution time are tabulated in Fig. 15. Our $Q_{content}$ needs 0.225 seconds in average to evaluate a stylized image with size of 512×512 . Although some metrics (e.g., GMSD, SSIM) are faster than $Q_{content}$, their prediction accuracy is not satisfactory, as demonstrated in Table II. Thus, it is apparent that the proposed $Q_{content}$ has the advantages in both high prediction accuracy and low time complexity.

2) *Performance Test on SR*: Obviously, the above FR-IQA methods are not suitable for quantitative evaluation of SR, because of the difference in contents between the stylized images and the style images. In addition, general NR-IQA methods are also ineffective because they lack a strong association (e.g., style pattern and brush stroke) with AST. To our best knowledge, there is no related methods for evaluating the quality of style images. Here, we only present the performance of the proposed Q_{style} on SR evaluation in Table III. It can be seen that the Q_{style} achieves the relatively good performance.

3) *Performance Test on OV*: Due to the lack of corresponding comparison methods, a strategy that incorporates the proposed Q_{style} with the existing FR-IQA methods is proposed to construct the comparison methods for evaluating OV quality. Specifically, the quality values of CP calculated by different FR-IQA methods are multiplied with Q_{style} , defined as:

$$\begin{cases} Q_{M*} = Q_{M\uparrow} \cdot Q_{style} \\ Q_{M*} = Q_{M\downarrow} \cdot (1 - Q_{style}) \end{cases} \quad (20)$$

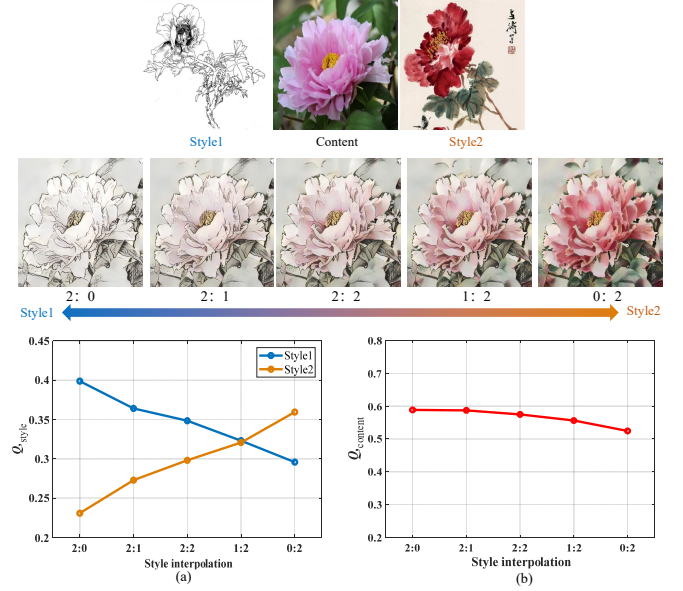


Fig. 17. Robustness analysis of the proposed Q_{style} and $Q_{content}$ in style interpolation application.

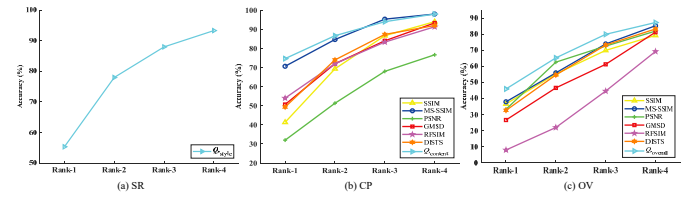


Fig. 18. Rank-n accuracy on the three quality factors.

where M denotes different FR-IQA method (e.g., SSIM [48], FSIM [38], MS-SSIM [65], IW-SSIM [37], Peak Signal-to-Noise Ratio (PSNR), MAD [66], VIF [36], VSI [39], GMSD [67], UQI [68], IFC [69], RFSIM [70] or DISTS [56]), $Q_{M\uparrow}$ (or $Q_{M\downarrow}$) denotes the higher (or lower) value for a better CP quality, calculated by each FR-IQA method, and Q_{M*} denotes the final OV quality generated by incorporating $Q_{M\uparrow}$ (or $Q_{M\downarrow}$) and Q_{style} .

The performance results of each are shown in Table IV. From this table, we observe that: 1) All the FR-IQA methods have achieved good compatibility with our Q_{style} , and most of them have SRCC values larger than 0.4. 2) Obviously, our proposed $Q_{overall}$ via a combination of Q_{style} and $Q_{content}$ achieves the best performance and outperforms other metrics by a large margin. Actually, as discussed in Section III-D, there still leaves a large space for improving the evaluation accuracy via proper importance weights and combination strategy.

D. Robustness Analysis

In this section, we present the robustness of our proposed Q_{style} and $Q_{content}$ in two AST applications (i.e., content-style trade-off and style interpolation) which are included in many AST methods.

1) *Content-style trade-off*: This application can adjust the degree of stylization. Three style degree groups with smooth












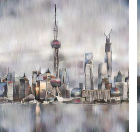
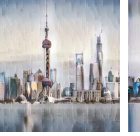
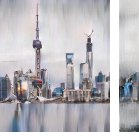
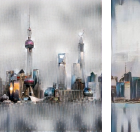
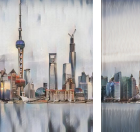
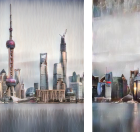
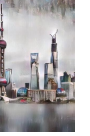
A									
	Method	SEM	LST	MST	MANet	AdaIN	SANet	AAMS	WCT
	SR*	1	2	3	4	5	6	7	8
	OR*	2	4	5	3	6	1	8	7
B									
	Method	WCT	MST	AdaIN	SANet	AAMS	MANet	LST	SEM
	SR*	1	2	3	4	5	6	7	8
	OR*	6	7	5	1	8	3	4	2

Fig. 19. Some typical failure ranking of our method on the OV evaluation.

changes generated by MANet [27] are presented in Fig. 16. When $\alpha = 1$, the fully stylized image is obtained. Fig. 16 (a)-(b) present $Q_{content}$ and Q_{style} results with different degrees of stylization. It can be seen that as α increases from 0 to 1, the $Q_{content}$ (or Q_{style}) value is consequently decreasing (or increasing) gradually which indicates that our Q_{style} and $Q_{content}$ can effectively capture the changes in the style patterns and content structure of the image.

2) *Style interpolation*: This application is to merge multiple style images into a single generated result. Here, we also utilize MANet [27] to generate a group of stylized images with different interpolations, and then use Q_{style} (or $Q_{content}$) to evaluate SR (or CP) of the stylized images. As shown in the Fig. 17 (a), with the continuous decline of the weights for the specific styles, the Q_{style} value is consequently decreasing gradually which indicates that our Q_{style} can clarify style characteristics and accurately evaluate SR even under the interference of multiple styles. Fig. 17 (b) presents that our $Q_{content}$ gives almost the same value to the different style interpolation images, which proves the robustness of $Q_{content}$.

E. Ranking Capability

1) *Performance Test on Rank-n accuracy*: To comprehensively compare the performance of the IQA metrics, we also focus on the performance of Rank-n accuracy [71]. Given the eight stylized images for each Content-Style image pair, the rank-n accuracy is the percentage of the objective scores where the subjective-rated best one is within their top n positions. The results are presented in Fig. 18. We can observe that the proposed method achieves fairly good performance in the SR, CP and OV ranking accuracy tests. Since one of the most important applications of AST-IQA metric is to guide the generation of stylized images, the proposed method is a promising tool for automatic selection of the optimal transferring result from a set of candidates.

2) *Failure Ranking Analysis*: As aforementioned, we demonstrate the ranking capability of the proposed method on

the three quality factors. However, in some special situations, the proposed method encounters challenges to achieve the expected ranking results. As shown in Fig. 19, we present two group representative failure ranking on the OV evaluation, which can be divided into two categories. In the first category, our method fails to capture extraneous artifacts, as shown in Fig. 19 (A). We select the stylization produced by SANet [23] as the optimal result, which produces unpleasing eye-like artifacts (zoom in for greater clarity) due to the fine-grained nature. The reason behind this lies in that our method mainly uses global sparse representation and ignores the local extraneous artifacts. In the second category, our method fails to effectively balance the importance of quality factors, as show in Fig. 19 (B). Actually, the CP and SR do not always complement each other. A non-realistic style leads to lower content retention in the final stylization result. Obviously, there is a large room to manipulate the importance weights for the quality factors. Overall, how to further dig the aesthetic information behind the stylization and propose a better strategy to balance different quality factors are the key issues to be explored in the future work.

V. CONCLUSION

In this paper, we first constructed a new database (AST-IQAD) to collect the subject-rated scores on the three quality factors of CP, SR, and OV. Then, a new sparse representation-based image quality evaluation metric (SRQE) is proposed to predict the human perception toward different stylized results. Experimental results show that our proposed method produces very promising AST-IQA results, which significantly outperforms many existing general purpose IQA methods. Overall, our new database creates a reliable platform to evaluate the performance of different AST algorithms and our method is helpful for guiding the design of different algorithms. In our future work, we will further mine the aesthetic information behind the stylization and propose a better strategy to balance different quality factors.

REFERENCES

- [1] Y. Jing, Y. Yang, Z. Feng, J. Ye, Y. Yu, and M. Song, "Neural style transfer: A review," *IEEE transactions on visualization and computer graphics*, vol. 26, no. 11, pp. 3365–3385, 2019.
- [2] A. A. Efros and W. T. Freeman, "Image quilting for texture synthesis and transfer," in *Proceedings of the 28th annual conference on Computer graphics and interactive techniques*, 2001, pp. 341–346.
- [3] V. Kwatra, I. Essa, A. Bobick, and N. Kwatra, "Texture optimization for example-based synthesis," in *ACM SIGGRAPH 2005 Papers*, 2005, pp. 795–802.
- [4] L. A. Gatys, A. S. Ecker, and M. Bethge, "Image style transfer using convolutional neural networks," in *Proceedings of the IEEE conference on computer vision and pattern recognition*, 2016, pp. 2414–2423.
- [5] J. Cheng, A. Jaiswal, Y. Wu, P. Natarajan, and P. Natarajan, "Style-aware normalized loss for improving arbitrary style transfer," in *Proceedings of the IEEE/CVF Conference on Computer Vision and Pattern Recognition*, 2021, pp. 134–143.
- [6] S. Liu, T. Lin, D. He, F. Li, M. Wang, X. Li, Z. Sun, Q. Li, and E. Ding, "Adaattn: Revisit attention mechanism in arbitrary neural style transfer," in *Proceedings of the IEEE/CVF international conference on computer vision*, 2021, pp. 6649–6658.
- [7] H. Chen, L. Zhao, Z. Wang, H. Zhang, Z. Zuo, A. Li, W. Xing, and D. Lu, "Dualast: Dual style-learning networks for artistic style transfer," in *Proceedings of the IEEE/CVF Conference on Computer Vision and Pattern Recognition*, 2021, pp. 872–881.
- [8] L. A. Gatys, A. S. Ecker, M. Bethge, A. Hertzmann, and E. Shechtman, "Controlling perceptual factors in neural style transfer," in *Proceedings of the IEEE conference on computer vision and pattern recognition*, 2017, pp. 3985–3993.
- [9] Y. Li, N. Wang, J. Liu, and X. Hou, "Demystifying neural style transfer," *arXiv preprint arXiv:1701.01036*, 2017.
- [10] E. Risser, P. Wilmot, and C. Barnes, "Stable and controllable neural texture synthesis and style transfer using histogram losses," *arXiv preprint arXiv:1701.08893*, 2017.
- [11] N. Kolkin, J. Salavon, and G. Shakhnarovich, "Style transfer by relaxed optimal transport and self-similarity," in *Proceedings of the IEEE/CVF Conference on Computer Vision and Pattern Recognition*, 2019, pp. 10 051–10 060.
- [12] L. Du, "How much deep learning does neural style transfer really need? an ablation study," in *Proceedings of the IEEE/CVF Winter Conference on Applications of Computer Vision*, 2020, pp. 3150–3159.
- [13] L.-Y. Wei and M. Levoy, "Fast texture synthesis using tree-structured vector quantization," in *Proceedings of the 27th annual conference on Computer graphics and interactive techniques*, 2000, pp. 479–488.
- [14] T. Q. Chen and M. Schmidt, "Fast patch-based style transfer of arbitrary style," *arXiv preprint arXiv:1612.04337*, 2016.
- [15] S. Gu, C. Chen, J. Liao, and L. Yuan, "Arbitrary style transfer with deep feature reshuffle," in *Proceedings of the IEEE Conference on Computer Vision and Pattern Recognition*, 2018, pp. 8222–8231.
- [16] J. Yoo, Y. Uh, S. Chun, B. Kang, and J.-W. Ha, "Photorealistic style transfer via wavelet transforms," in *Proceedings of the IEEE/CVF International Conference on Computer Vision*, 2019, pp. 9036–9045.
- [17] Z. Wang, L. Zhao, H. Chen, L. Qiu, Q. Mo, S. Lin, W. Xing, and D. Lu, "Diversified arbitrary style transfer via deep feature perturbation," in *Proceedings of the IEEE/CVF Conference on Computer Vision and Pattern Recognition*, 2020, pp. 7789–7798.
- [18] G. Ghiasi, H. Lee, M. Kudlur, V. Dumoulin, and J. Shlens, "Exploring the structure of a real-time, arbitrary neural artistic stylization network," *arXiv preprint arXiv:1705.06830*, 2017.
- [19] X. Huang and S. Belongie, "Arbitrary style transfer in real-time with adaptive instance normalization," in *Proceedings of the IEEE international conference on computer vision*, 2017, pp. 1501–1510.
- [20] Y. Li, C. Fang, J. Yang, Z. Wang, X. Lu, and M.-H. Yang, "Universal style transfer via feature transforms," *Advances in neural information processing systems*, vol. 30, 2017.
- [21] F. Shen, S. Yan, and G. Zeng, "Neural style transfer via meta networks," in *Proceedings of the IEEE Conference on Computer Vision and Pattern Recognition*, 2018, pp. 8061–8069.
- [22] X. Li, S. Liu, J. Kautz, and M.-H. Yang, "Learning linear transformations for fast image and video style transfer," in *Proceedings of the IEEE/CVF Conference on Computer Vision and Pattern Recognition*, 2019, pp. 3809–3817.
- [23] D. Y. Park and K. H. Lee, "Arbitrary style transfer with style-attentional networks," in *proceedings of the IEEE/CVF conference on computer vision and pattern recognition*, 2019, pp. 5880–5888.
- [24] Y. Yao, J. Ren, X. Xie, W. Liu, Y.-J. Liu, and J. Wang, "Attention-aware multi-stroke style transfer," in *Proceedings of the IEEE/CVF Conference on Computer Vision and Pattern Recognition*, 2019, pp. 1467–1475.
- [25] Y. Zhang, C. Fang, Y. Wang, Z. Wang, Z. Lin, Y. Fu, and J. Yang, "Multimodal style transfer via graph cuts," in *Proceedings of the IEEE/CVF International Conference on Computer Vision*, 2019, pp. 5943–5951.
- [26] C. Chen, "Structure-emphasized multimodal style transfer," *Master-Tokyo Institute of Technology: Tokyo, Japan*, 2020.
- [27] Y. Deng, F. Tang, W. Dong, W. Sun, F. Huang, and C. Xu, "Arbitrary style transfer via multi-adaptation network," in *Proceedings of the 28th ACM international conference on multimedia*, 2020, pp. 2719–2727.
- [28] Y. Jing, X. Liu, Y. Ding, X. Wang, E. Ding, M. Song, and S. Wen, "Dynamic instance normalization for arbitrary style transfer," in *Proceedings of the AAAI Conference on Artificial Intelligence*, vol. 34, no. 04, 2020, pp. 4369–4376.
- [29] Y. Pang, J. Lin, T. Qin, and Z. Chen, "Image-to-image translation: Methods and applications," *IEEE Transactions on Multimedia*, 2021.
- [30] D. Chen, L. Yuan, J. Liao, N. Yu, and G. Hua, "Stylebank: An explicit representation for neural image style transfer," in *Proceedings of the IEEE conference on computer vision and pattern recognition*, 2017, pp. 1897–1906.
- [31] V. Dumoulin, J. Shlens, and M. Kudlur, "A learned representation for artistic style," *arXiv preprint arXiv:1610.07629*, 2016.
- [32] Y. Li, C. Fang, J. Yang, Z. Wang, X. Lu, and M.-H. Yang, "Diversified texture synthesis with feed-forward networks," in *Proceedings of the IEEE conference on computer vision and pattern recognition*, 2017, pp. 3920–3928.
- [33] M.-C. Yeh, S. Tang, A. Bhattad, and D. A. Forsyth, "Quantitative evaluation of style transfer," *arXiv preprint arXiv:1804.00118*, 2018.
- [34] Z. Wang, L. Zhao, H. Chen, Z. Zuo, A. Li, W. Xing, and D. Lu, "Evaluate and improve the quality of neural style transfer," *Computer Vision and Image Understanding*, vol. 207, p. 103203, 2021.
- [35] H. Chen, X. Chai, F. Shao, X. Wang, Q. Jiang, M. Chao, and Y.-S. Ho, "Perceptual quality assessment of cartoon images," *IEEE Transactions on Multimedia*, 2021.
- [36] H. R. Sheikh and A. C. Bovik, "Image information and visual quality," *IEEE Transactions on image processing*, vol. 15, no. 2, pp. 430–444, 2006.
- [37] Z. Wang and Q. Li, "Information content weighting for perceptual image quality assessment," *IEEE Transactions on image processing*, vol. 20, no. 5, pp. 1185–1198, 2010.
- [38] L. Zhang, L. Zhang, X. Mou, and D. Zhang, "Fsim: A feature similarity index for image quality assessment," *IEEE transactions on Image Processing*, vol. 20, no. 8, pp. 2378–2386, 2011.
- [39] L. Zhang, Y. Shen, and H. Li, "Vsi: A visual saliency-induced index for perceptual image quality assessment," *IEEE Transactions on Image processing*, vol. 23, no. 10, pp. 4270–4281, 2014.
- [40] A. K. Moorthy and A. C. Bovik, "A two-step framework for constructing blind image quality indices," *IEEE Signal processing letters*, vol. 17, no. 5, pp. 513–516, 2010.
- [41] A. Mittal, A. K. Moorthy, and A. C. Bovik, "No-reference image quality assessment in the spatial domain," *IEEE Transactions on image processing*, vol. 21, no. 12, pp. 4695–4708, 2012.
- [42] A. Mittal, R. Soundararajan, and A. C. Bovik, "Making a "completely blind" image quality analyzer," *IEEE Signal processing letters*, vol. 20, no. 3, pp. 209–212, 2012.
- [43] T. O. Aydin, A. Smolic, and M. Gross, "Automated aesthetic analysis of photographic images," *IEEE transactions on visualization and computer graphics*, vol. 21, no. 1, pp. 31–42, 2014.
- [44] D. Mould and P. L. Rosin, "Developing and applying a benchmark for evaluating image stylization," *Computers & Graphics*, vol. 67, pp. 58–76, 2017.
- [45] P. L. Rosin, T. Wang, H. Winnemöller, D. Mould, I. Berger, J. Collo-mosse, Y.-K. Lai, C. Li, H. Li, A. Shamir *et al.*, "Benchmarking non-photorealistic rendering of portraits," 2017.
- [46] Y. Huang, M. Jing, J. Zhou, Y. Liu, and Y. Fan, "Lccstyle: Arbitrary style transfer with low computational complexity," *IEEE Transactions on Multimedia*, 2021.
- [47] Z. Ma, J. Li, N. Wang, and X. Gao, "Image style transfer with collection representation space and semantic-guided reconstruction," *Neural Networks*, vol. 129, pp. 123–137, 2020.
- [48] Z. Wang, A. C. Bovik, H. R. Sheikh, and E. P. Simoncelli, "Image quality assessment: from error visibility to structural similarity," *IEEE transactions on image processing*, vol. 13, no. 4, pp. 600–612, 2004.
- [49] P. Resnick and H. R. Varian, "Recommender systems," *Communications of the ACM*, vol. 40, no. 3, pp. 56–58, 1997.

- [50] C. Li and T. Chen, "Aesthetic visual quality assessment of paintings," *IEEE Journal of selected topics in Signal Processing*, vol. 3, no. 2, pp. 236–252, 2009.
- [51] F. Gao, D. Tao, X. Gao, and X. Li, "Learning to rank for blind image quality assessment," *IEEE transactions on neural networks and learning systems*, vol. 26, no. 10, pp. 2275–2290, 2015.
- [52] R. I.-R. BT, "Methodology for the subjective assessment of the quality of television pictures," *International Telecommunication Union*, 2002.
- [53] R. A. Bradley and M. E. Terry, "Rank analysis of incomplete block designs: I. the method of paired comparisons," *Biometrika*, vol. 39, no. 3/4, pp. 324–345, 1952.
- [54] W.-S. Lai, J.-B. Huang, Z. Hu, N. Ahuja, and M.-H. Yang, "A comparative study for single image blind deblurring," in *Proceedings of the IEEE Conference on Computer Vision and Pattern Recognition*, 2016, pp. 1701–1709.
- [55] J. M. Hughes, D. J. Graham, and D. N. Rockmore, "Quantification of artistic style through sparse coding analysis in the drawings of pieter bruegel the elder," *Proceedings of the National Academy of Sciences*, vol. 107, no. 4, pp. 1279–1283, 2010.
- [56] K. Ding, K. Ma, S. Wang, and E. P. Simoncelli, "Image quality assessment: Unifying structure and texture similarity," *IEEE transactions on pattern analysis and machine intelligence*, 2020.
- [57] J. Mairal, F. Bach, J. Ponce, and G. Sapiro, "Online dictionary learning for sparse coding," in *Proceedings of the 26th annual international conference on machine learning*, 2009, pp. 689–696.
- [58] F. Shao, K. Li, W. Lin, G. Jiang, M. Yu, and Q. Dai, "Full-reference quality assessment of stereoscopic images by learning binocular receptive field properties," *IEEE Transactions on Image Processing*, vol. 24, no. 10, pp. 2971–2983, 2015.
- [59] N. Ponomarenko, O. Ieremeiev, V. Lukin, K. Egiazarian, L. Jin, J. Astola, B. Vozel, K. Chehdi, M. Carli, F. Battisti *et al.*, "Color image database tid2013: Peculiarities and preliminary results," in *European workshop on visual information processing (EUVIP)*. IEEE, 2013, pp. 106–111.
- [60] T. Lindeberg, "Scale-space theory: A basic tool for analyzing structures at different scales," *Journal of applied statistics*, vol. 21, no. 1-2, pp. 225–270, 1994.
- [61] D. G. Lowe, "Distinctive image features from scale-invariant keypoints," *International journal of computer vision*, vol. 60, no. 2, pp. 91–110, 2004.
- [62] Y. Fu, H. Zeng, L. Ma, Z. Ni, J. Zhu, and K.-K. Ma, "Screen content image quality assessment using multi-scale difference of gaussian," *IEEE Transactions on Circuits and Systems for Video Technology*, vol. 28, no. 9, pp. 2428–2432, 2018.
- [63] B. Hu, L. Li, H. Liu, W. Lin, and J. Qian, "Pairwise-comparison-based rank learning for benchmarking image restoration algorithms," *IEEE Transactions on Multimedia*, vol. 21, no. 8, pp. 2042–2056, 2019.
- [64] Z. Peng, Q. Jiang, F. Shao, W. Gao, and W. Lin, "Lgpd+: Image retargeting quality assessment by measuring local and global geometric distortions," *IEEE Transactions on Circuits and Systems for Video Technology*, 2021.
- [65] Z. Wang, E. P. Simoncelli, and A. C. Bovik, "Multiscale structural similarity for image quality assessment," in *The Thirty-Seventh Asilomar Conference on Signals, Systems & Computers*, 2003, vol. 2. Ieee, 2003, pp. 1398–1402.
- [66] E. C. Larson and D. M. Chandler, "Most apparent distortion: full-reference image quality assessment and the role of strategy," *Journal of electronic imaging*, vol. 19, no. 1, p. 011006, 2010.
- [67] W. Xue, L. Zhang, X. Mou, and A. C. Bovik, "Gradient magnitude similarity deviation: A highly efficient perceptual image quality index," *IEEE transactions on image processing*, vol. 23, no. 2, pp. 684–695, 2013.
- [68] Z. Wang and A. C. Bovik, "A universal image quality index," *IEEE signal processing letters*, vol. 9, no. 3, pp. 81–84, 2002.
- [69] H. R. Sheikh, A. C. Bovik, and G. De Veciana, "An information fidelity criterion for image quality assessment using natural scene statistics," *IEEE Transactions on image processing*, vol. 14, no. 12, pp. 2117–2128, 2005.
- [70] L. Zhang, L. Zhang, and X. Mou, "Rfsim: A feature based image quality assessment metric using riesz transforms," in *2010 IEEE International Conference on Image Processing*. IEEE, 2010, pp. 321–324.
- [71] Y. Zhang, W. Lin, Q. Li, W. Cheng, and X. Zhang, "Multiple-level feature-based measure for retargeted image quality," *IEEE Transactions on Image Processing*, vol. 27, no. 1, pp. 451–463, 2017.